mental resolution is close to 1 μ over the whole area. Figure 3 is a (111)-reflection topograph taken with CoK_β characteristic radiation, showing stacking fault tetrahedra in a 15-μ thick epitaxial layer of silicon. The instrumental resolution varied from 0.1 to 2 μ over the 4-cm² area photographed. For the small area shown here the instrumental resolution is 0.5 μ. A Kodak high resolution plate was used to record the finest details.

Up to now it has been implied in the literature that to obtain high-resolution topographs of large-area crystals it is necessary to reduce the effective source size to eliminate the $K_{\alpha 1}$–$K_{\alpha 2}$ interference, and then scan the beam over the desired surface. In this paper it is shown that the use of K_β radiation permits the use of a larger effective beam size, thus making it possible to sample a larger area without recourse to scanning. In addition, it is shown that the exposure time required to photograph equal areas is shorter using the K_β characteristic radiation. These two advantages are combined in a technique which is faster, simpler, and less expensive than other x-ray topographic techniques.

* This work was supported in part by the Defense Research Board of Canada through its Directorate of Industrial Research.

[1] A. R. Lang, Acta. Cryst. **12**, 249 (1959).

[2] J. K. Howard and R. H. Cox, *Advances in X-ray Analysis* (Plenum Press, Inc., New York, 1965), p. 35.

[3] K. A. Carlson and R. Wegener, J. Appl. Phys. **32**, 125 (1961).

[4] W. W. Webb, *Direct Observation of Imperfections in Crystals*, J. B. Newkirk and J. H. Wernick, Eds. (Interscience Publishers, New York, 1962), p. 67.

[5] A. R. Lang, in *Encyclopedia of X-rays and Gamma Rays*, G. L. Clark Ed. (Reinhold Publishing Corp., Inc., New York, 1963), p. 1053.

[6] G. H. Schwuttke, J. Appl. Phys. **33**, 2760 (1962).

[7] J. H. Williams, Phys. Rev. **44**, 146 (1933).

[8] The slit S_2 of width $M_2=\Delta\theta_{\lambda_1\lambda_2}d_2$ is used to prevent the reflection of the λ_1 and the λ_2 components from two different areas of the sample respectively. Since in general $d_1 \leqq d_2$, $M_1 \leqq M_2$ and f is determined by the smaller of M_1/H and 1. See also Ref. 4.

Amorphous Ferromagnetic Phase in Iron–Carbon–Phosphorus Alloys*

POL DUWEZ AND S. C. H. LIN
W. M. Keck Laboratory of Engineering Materials, California Institute of Technology, Pasadena, California
(Received 1 May 1967)

A limited number of amorphous alloys have been obtained by rapid cooling from the liquid state. These include Au–Si,[1] Pd–Si,[2] Pd–Ge, Pt–Si, Pt–Ge, Pt–Sb, and Rh–Ge.[3] In all these systems, armorphous alloys can be obtained within a rather narrow range of concentrations in the vicinity of the eutectic composition. In all systems, the eutectric temperature is also very low with respect to the melting point of the main component in the alloy. According to Cohen and Turnbull,[4,5] this particular feature of an equilibrium diagram is conducive to glass formation. Although other factors must play a role in retarding the crystallization of liquid alloys, the existence of a "deep eutectic" in the phase diagram is certainly an important condition since in all cases reported so far this condition has been satisfied.

When the search for an amorphous iron-base alloy was initiated, it was recognized that phosphorus would be an interesting alloying element since the eutectic temperature is low (1050°C) compared to the melting point of iron (1534°C). Binary Fe–P alloys of near eutectic composition (17.5 at.% P) were not entirely amorphous after quenching. The addition of carbon (which probably further depresses the eutectic temperature) resulted in an amorphous structure. Although the amorphous phase can be obtained within a certain range of compositions, most of the alloys studied (and analyzed after quenching) contained approximately 6.0 wt% P and 1.7 wt% C.

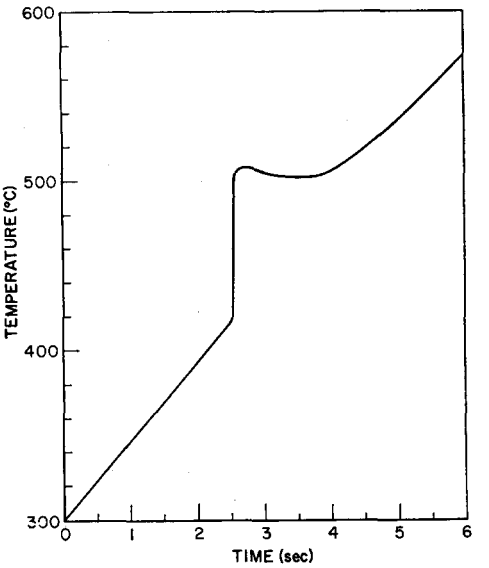

FIG. 1. Temperature vs time curve of an amorphous foil of Fe–P–C alloy.

The alloys were prepared by mixing the elemental powders and compacting under a pressure of 50 000 lb/in². The compacts were sealed under vacuum in fused-quartz vials and heated up to about 580°C (10°C below the phosphorus melting point) at a rate not exceeding 50°C/h. After about 24 h, the temperature was increased to 600°C and kept constant for about 24 h. After this heat treatment, an x-ray diffraction pattern of the compact indicated that most of the phosphorus was combined into Fe_3P. The specimens were then reheated to about 900°C and kept at that temperature for at least 24 h.

Rapid quenching from the liquid state was achieved by the "piston and anvil" technique.[6] The quenched foils were from 20 to 25 mm in diameter and about 50 μ in thickness. The diffraction patterns of these foils, taken with either a diffractometer or a powder camera and using Mo K_α radiation monochromatized by the (200) reflection of a LiF crystal, showed three very broad peaks at 2θ angles of 19.8°, 33.7° and 49.5°. The results of transmission electronmicroscopy and electron diffraction were similar to those previously reported for Pd–Si alloys,[2] namely complete lack of contrast in microscopy and existance of three very broad diffraction rings.

As in the case of Pd–Si, the Fe–P–C amorphous phase transformed very rapidly into the equilibrium crystalline phases (α Fe–C solid solution, Fe_3P and Fe_3C) when heated at rates exceeding about 100°C/min. Under these conditions a sudden release of heat can be detected by thermal analysis and a typical temperature-vs-time curve is shown in Fig. 1. The temperature increase due to the amorphous to crystalline transition corresponds to approximately 900 cal/mole. The fact that the alloy suddenly transforms around 420°C when heated rapidly enough does not mean that the amorphous structure is stable up to that temperature and nucleation and growth of the crystalline phases will of course proceed at certain rates below 420°C. From the results obtained so far in a study of the kinetics of crystallization, it appears that at 350°C the amorphous phase is stable for at least 24 h.

The Fe–P–C amorphous phase is ferromagnetic. This is not too surprising since it has been shown by Gubanov[7] that ferromagnetism does not require a crystal structure. The hysteresis cycle of quenched foils is typical of a soft ferromagnetic alloy with a saturation magnetization of about 6.8 kG and a coercive force of approximately 3 Oe. The Curie temperature (measured by the induction method) is 320°C. These characteristics are likely to vary from specimen to specimen because of difficulties

in avoiding evaporation of phosphorus and oxidation of carbon in preparing the alloys. In addition, as explained in Ref. 6, the quenching conditions in the piston and anvil technique cannot be controlled accurately enough to insure reproducibility of the rate of cooling and hence, the fine details of the atomic arrangement in the amorphous structure may vary from specimen to specimen.

The authors wish to thank J. C. Russ of the Bethlehem Steel Research Laboratory, Bethlehem, Pennsylvania, for providing the chemical analysis of the alloys.

* Work sponsored by the U. S. Atomic Energy Commission.

[1] W. Klement, Jr., R. H. Willens, and Pol Duwez, Nature **187**, 869 (1960).
[2] Pol Duwez, R. H. Willens, and R. C. Crewdson, J. Appl. Phys. **36**, 2267 (1965).
[3] R. C. Crewdson, Ph.D. thesis, California Institute of Technology, (1966).
[4] M. H. Cohen and D. Turnbull, Nature **189**, 131 (1961).
[5] D. Turnbull, Trans. Met. Soc. AIME **221**, 422 (1961).
[6] Pol Duwez, in *Progress in Solid State Chemistry*, H. Reiss, Ed. (Pergamon Press, London 1966), Vol. 3, p. 377.
[7] A. I. Gubanov, Soviet Phys.—Solid State **2**, 468 (1960).

Turbulent Effects in the Formation of Buoyant Vortex Rings*

TIMOTHY FOHL
Mt. Auburn Research Associates, Inc., Cambridge, Massachusetts
(Received 13 March 1967; in final form 31 May 1967)

In this communication we discuss the process in which a mass of buoyant fluid released from rest forms a buoyant vortex ring.

The theory of buoyant vortex rings as elucidated by Turner has proven useful in interpreting the motion of very buoyant fluids such as those encountered in atmospheric nuclear bursts.[1,2] Turner's arguments are based on the assumption that the circulation K, of the vortex ring remains constant during the lifetime of the fully formed ring. Equation (1), which is due to Bjerknes, relates the rate of change of circulation inside a closed path of integration to the density and pressure along the line enclosing the region.[3] The fluid density is denoted by ρ.

$$dK/dt = -\int \rho^{-1} \operatorname{grad} p \cdot ds, \tag{1}$$

and p is the local pressure. When the buoyant fluid in a vortex ring is confined to a ring-shaped volume, the path of integration of Eq. (1) can pass through the hole in the ring and return through the ambient fluid without passing through any regions containing buoyant fluid. The integral reduces to zero when integrated over this path, and the circulation included in the integration loop, i.e., the circulation of ring, remains constant. However, when a spherical mass of buoyant fluid is released, the integral of Eq. (1) is not zero if a part of the integration path passes through the buoyant mass. Circulation will be generated by buoyancy forces until a fully formed vortex ring results.

Turner has shown that a buoyant vortex ring will expand as it rises with its radius R, proportional to the height h it rises. That is, $dR/dh = \alpha$, where α is a constant determined by the initial conditions.[1] The buoyancy force acting on the fluid mass is ρF, where F is given by

$$F = gW(\rho - \rho')/\rho. \tag{2}$$

The volume of the buoyant fluid is W, g is the acceleration of gravity, ρ' is the density of the buoyant fluid, and ρ is the density of the surrounding fluid. The spreading coefficient α is given in terms of the buoyancy and the vortex-ring parameters by

$$\alpha = F/2\pi C_2 K^2, \tag{3}$$

where C_2 is a shape-dependent constant. The kinetic energy of the ring T, is given by

$$T = C_1 \rho K^2 R, \tag{4}$$

with C_1 a constant dependent on the shape of the ring.[4] These equations pertain to the motion of the fully formed buoyant vortex ring, and we now discuss the factors which relate the parameters of these equations to the initial size and buoyancy of a mass of fluid released from rest.

Consider the case of a spherical mass of buoyant fluid released instantaneously and without any initial momentum. The fluid rises and transforms into a vortex ring by the time its center of mass rises a distance h_1. Assume that $h_1 = C_3 R_0$ where R_0 is the radius of the original buoyant sphere, and C_3 is a constant for all vortex rings formed in this manner. By the time the buoyant fluid has formed a fully developed vortex ring it has lost potential energy equal to $\rho F h_1$. If all this energy appears as kinetic energy of the vortex ring, Eq. (3) yields

$$F h_1 = C_1 K^2 R_1, \tag{5}$$

where R_1 is the radius of the vortex ring at the end of the formation phase.

Equations (4) and (5) can be used to find an expression for α:

$$\alpha = (C_1/2\pi C_2 C_3)(R_1/R_0). \tag{6}$$

If the deformation of a spherical mass of buoyant fluid into a vortex ring proceeded in a regular and reproducible way, the parameters of the vortex ring could be readily predicted from the initial conditions. The constant C_1 and C_2 are calculable, and C_3 and R_1/R_0 can be determined from experiments. However, turbulent eddies occurring during ring formation introduce a random factor in the ratio R_1/R_0 which is difficult to predict.

The effect of eddies is to increase the radius of the vortex ring over the radius which it would have if the formation took place with no random eddies present. If a smooth formation yields a ring of radius R_1', the ring will have radius $R_1 = R_1' + l$ when eddies occur during the formation phase. The length l is a length characteristic of size of the eddies which protrude from the envelope of the evolving vortex ring. The equation for α can be written as

$$\alpha = (C_1/2\pi C_2 C_3)(R_1'/R_0 + l/R_0). \tag{7}$$

The constants C_1, C_2, C_3, and R_1'/R_0 are determinable and remain constant in all releases of buoyant fluid. The random factor which causes the variations of vortex ring characteristics from release to release is contained in l. The length l is roughly the size of the larger edides although no well-defined relationship exists which connects l with measurements of eddy size. The eddy size depends sensitively on the size of irregular motions of the buoyant fluid at the moment of release as well as on the densities of the buoyant fluid and the surrounding fluid. The uncertain nature of the occurrence and growth of these eddies results in large variations in the characteristics of vortex ring formed by the release of buoyant fluid, even when the original conditions of density and size are kept constant. Since there is no relation which connects a measurement of eddy size to a value of l, we are limited to the qualitative statement that the larger the eddies, the larger l, and hence α will be. Because eddies occur in a random way, a series of releases in which larger eddies occur will show larger variation in α from release to release as well as a larger average value of α.

In order to test these ideas we carried out a series of model experiments. A mass of light gas mixed with smoke was released and its motion recorded by photographing it against a grid with periodic light flashes and an open shutter camera. Measurements of size and position as a function of time were made from the resulting photographs. The buoyant gas was released by bursting a soap bubble containing the mixture. On occasion very smooth releases were obtained. We used a very light gas consisting of a helium–air mixture in the hope that the motion would be stable against Rayleigh–Taylor instabilities when circulating, and that a smoother flow would result. This stabilization apparently is